2 Experimental part: Methods, Reagents, Syntheses

The experiments done in behalf of this thesis, due to the high cleanliness demands of the application, were undertaken with a serious consideration of chemical purity and clean environment.

2.1 Environments

All substrate washing, spin-coating and ITO passivation dipping procedures were performed in a Laminar-flow Box from Micro CleanRoom Technology GmbH with an "Astrocell II®" air cleaning facility.

Applications which needed protection from humidity or air oxygen have been performed in an InterTec GmbH Glove Box, under nitrogen gas with impurities less than 1 ppm.

Evaporation of organic substances for the production of solar cells has been done in a Balzers ultra-high-vacuum (UHV) evaporation chamber under pressure of about 10^{-7} mbar.

Chemical synthetic preparations, sensitive to humidity have been performed in a fume hood, with glassware under nitrogen gas flow.

2.2 Chemicals, reagents and materials

Chemicals used for cell preparation through UHV evaporation: ZnPc, C60 and BCP, were delivered from the company Covion. They had highest purity grade: 99%.

Other chemicals, used for ITO passivations were delivered from Sigma-Aldrich with a grade "Pure for analysis".

Chemicals from the sources mentioned above were used without further purification.

Chemicals synthesized by us were cleaned as described in synthesis (2.6.2).

Indium-Tin Oxide glass substrates were delivered by Präzisions Glas & Optic GmbH, readily cut in the desired size. The conducting oxide has been sputtered on polished float glass. Substrates used in the present work had a square resistance of 5, 10, 20, 50 and 100 Ω. For a standard solar cell, only 5 Ω/ glass was used for reproducibility.

PEDOT:PSS for spincoating on ITO was obtained from A. C. Starck (BAYER) with no further notice about purity, ingredients, composition.

2.3 Cleaning procedure for ITO

ITO, as received, is of course too contaminated for the purposes of solar cell production. That is why it needs to pass a thorough cleaning procedure to ensure that its surface is clean and more important - dust free. This cleaning procedure was applied as follows:

1. The ITO substrates after being wiped with absolute ethanol are placed in a beaker and ultrasonically cleaned for 20 minutes with acetone.
2. After that the solvent is being changed to 2-propanole and again 20 minutes in the ultrasonic bin are applied.
3. Then, after rinsing each piece of ITO glass with deionized water (MILLIPORE®), 2 different soap solutions from N. Bucher AG are being applied for further 20 minutes each in the ultrasonic bin.
4. Subsequently substrates were rinsed with plenty of deionized water and then dried, using ionized nitrogen gas gun.

Further no plasma or any other surface treatments were applied due to the fact that these change the surface work function of ITO [**23**,**24**]. For reproducibility all ITO substrates used in the current work were cleaned using the same cleaning procedure, described above. After the cleaning procedure the ITO substrates were used immediately, to avoid recontamination by storage.

2.4 ITO Passivations

ITO passivations applied in the current work are mostly wet dippings with exception of 8-Hydroxyquinoline which is a gas phase deposition and ZnO/Soluble Phthalocyanine which is an electrodeposition product.

The dipping solutions had the following concentrations:

- HCl 1M
- H_3PO_4 1M,
- HIO_4 1M,
- NH_3 1M,
- Zinc Phthalocyaninetetraphosphonic acid ($ZnPc(PO_3H)_4$) 10^{-4}M.

Deposition of 8-Hydroxyquinoline will be described in 2.6.1.

Co-electrodeposition of ZnO and $CuPc(SO_3H)_4$ was carried out of a mixed solution with concentrations: 0,1M $Zn(NO_3)_2$ and 5.10^{-4}M $CuPc(SO_3H)_4$ at a voltage of -1,1V at 70ºC for different time durations, depending on the desired thickness [**25**].

2.5 Conventional treatment – PEDOT:PSS Spin-coating

Coating ITO substrates with PEDOT:PSS was performed on a Delta 6RC spin-coater. The PEDOT:PSS solution, as received was too concentrated, that is why it was additionally diluted with deionized water to 60%, 70%, 80% and 90%. Different concentrations of this material yield also different thicknesses, which is anyway irrelevant to the current work. The highest cell efficiency was yielded with 70% concentration, so any reference to a cell with PEDOT:PSS will be done for this concentration. After applying the PEDOT:PSS solution on the ITO glass substrate it was pre-spinned at 200 rpm for 10 seconds, so that the complete surface gets covered with the solution. Then the spinning is continued at 2000 rpm to let the substrate dry. After this the substrate is heated 15 minutes at 100ºC to let the PEDOT:PSS dry and bind to the surface.

2.6 Syntheses

2.6.1 8-Hydroxyquinoline deposition

For the deposition of 8-Hydroxyquinoline on the surface of ITO a two stage process was used [**26**,**27**] (see reaction scheme – Figure 4), where in each reaction only the first monolayer reacts with the substrate. The first reaction was the deposition of a bridging molecule, followed by the 8-hydroxyquinoline after that. The natural OH-passivation of ITO [**28**] was used for the first step.

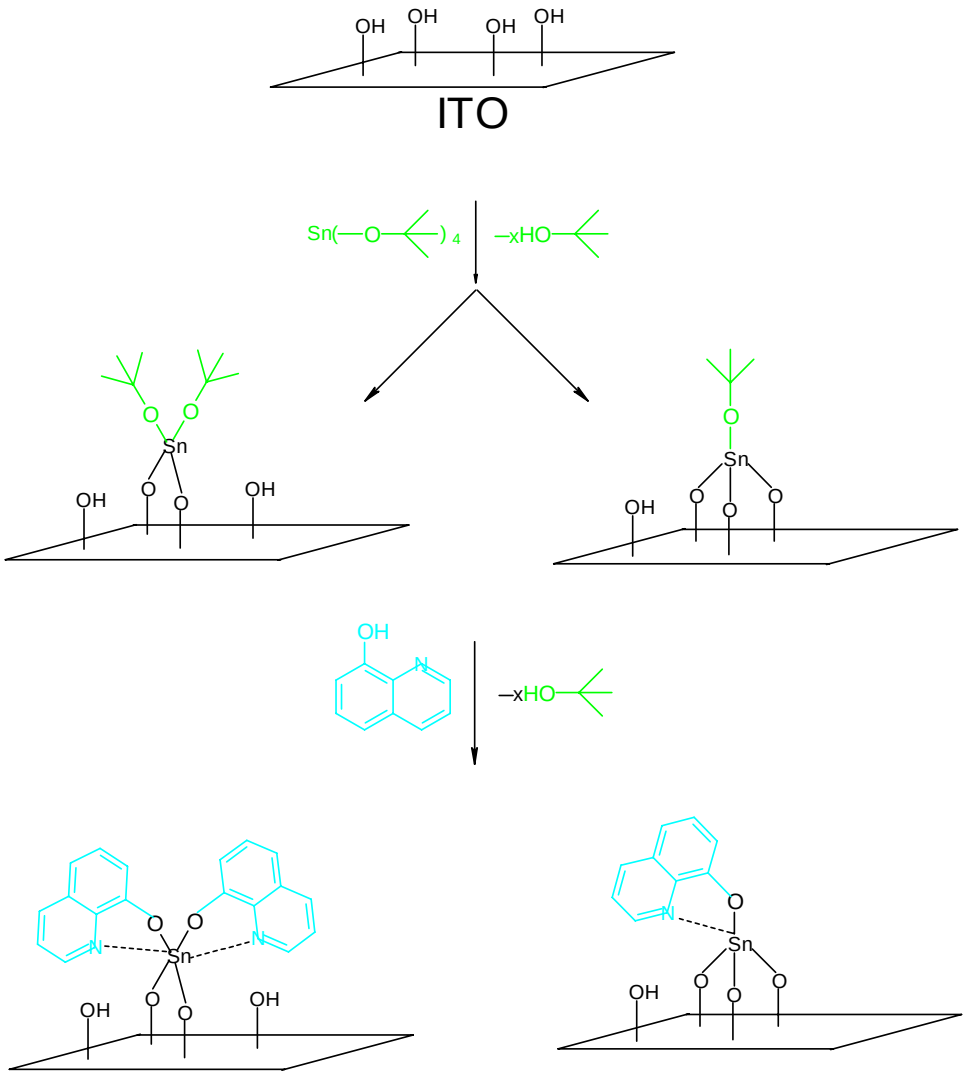

Figure 3. Two stage reaction of passivating ITO with 8-Hydroxyquinoline. At the first stage, a monolayer of tetra(tert-butoxy)tin is deposited on the surface, which is then used for the second reaction, for depositing a monolayer of 8-hydroxyquinoline

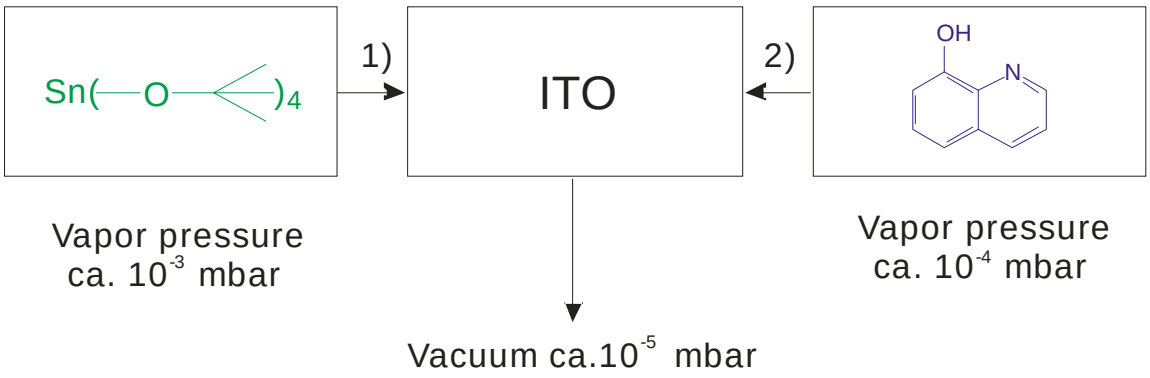

Figure 4. Schematic representation of the vacuum sublimation reaction apparatus. Reactions 1) and 2) are done one after another. Complete pumping of the chamber, between reactions, ensures no residual substance or multiple layer coverage

At moderate vacuum of about 10^{-5} mbar, a vent, connecting the precursor chamber and the substrate chamber, was opened. At room temperature, a flow of subliming Tetra(tert-butoxy)tin, reacted with the pre-cleaned ITO-glass sample. After 30 minute flow, the reaction chamber was isolated from the precursor and evacuated until no change in vacuum was to be observed, to assure the removal of excess substance, deposited on the surface, and the tert-butanol, a product of the reaction. Then the second reaction was carried out, again for 30 minutes in a flow of 8-Hydroxyquinoline. Afterwards once more the chamber was evacuated until there was no change in vacuum to ensure the evacuation of all quinoline, which is not chemically bound to the surface.

2.6.2 Zinc-Phthalocyaninetetraphosphonic acid synthesis

The synthesis of zinc-phthalocyaninetetraphosphonic acid was conducted as described elsewhere [**29**], with slight modifications. As starting material bromophthalodinitril was used. The conversion was made in three reaction stages.

3,4-Dicyanobenzophosphonic acid, diethyl ester

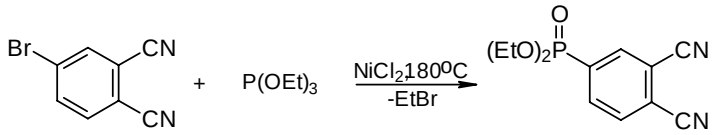

4-Bromophthalonitrile (3,1 g) is mixed with water free $NiCl_2$ (0,195 g) in a flask, fitted for direct distillation, and heated. At 180°C (and not 160 as described in the literature source) $P(OEt)_3$ (3,42 ml) is dropped to the melt. The forming EtBr distills in the same time with the weak N_2 flow. After the addition the mixture is being stirred one more hour at 180 degrees. In the end of the reaction the black reaction mixture is passed through a column of silica gel with chloroform as eluent (flash chromatography). The solvent is then distilled at a rotational evaporator. The product is vacuum distilled (0,3Torr) at about 190°C as a colorless liquid. Yield: 60%.

Zn-Phthalocyaninetetraphosphonic acid - diethyl ester,

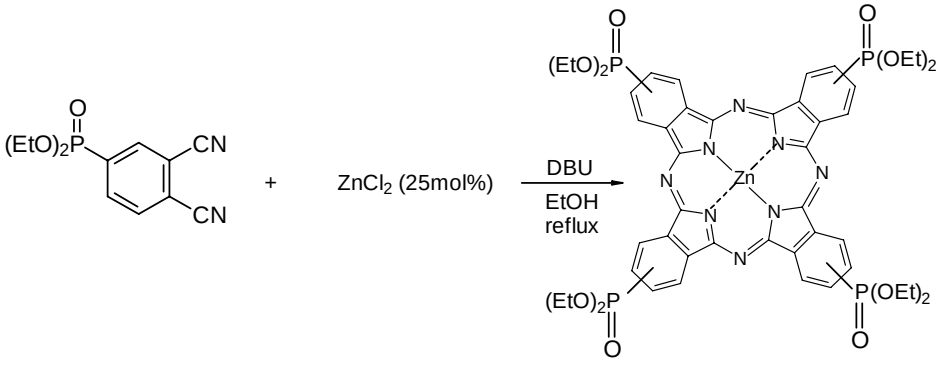

0,55 g of the precursor, 0,32 ml 1,8-Diazabicyclo[5.4.0]undec-7-ene (DBU79) and 71mg water-free $ZnCl_2$ are refluxed 40h in 35 ml abs. EtOH. After distillation of the solvent, the reaction mixture is being chromatographed on silica gel with Chloroform/Methanol (v:v=4:1). After vacuum evaporation of the solvents purple-blue powder is yielded (35% of the theoretical yield). T_{melt} >300°C.

Zinc-Phthalocyaninetetraphosphonic acid

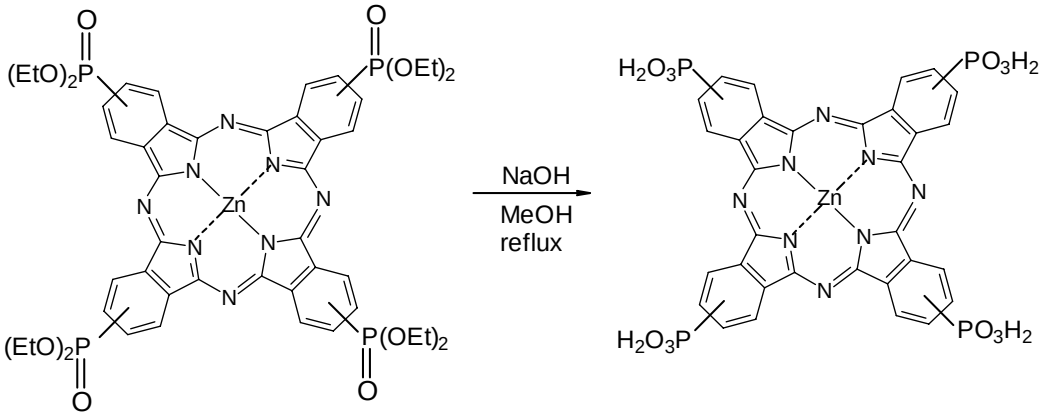

The ester is boiled with NaOH in methanol for 20h. After that the solvent is distilled at a rotation-distiller. With HCl the rest is led to a lower pH. The blue slurry is filtered. Recrystallization out of Methanol leads to blue crystals. Dimethylformamide (DMF)/Water (v:v=97:3) recommended in the literature reference as solvent for

recrystallization makes crystallization difficult, because of too high material solubility. Yield 90%.

Here it has to be mentioned, that a synthesis out of bromophthalonitril was also attempted. If the molar ratios are kept the same then the reactions can be conducted successfully and the subsequent substance is yielded. The temperature for the first substitutional reaction with bromophthalonitril is also 180°C and not 160°C, as mentioned in the literature source.

2.7 Solar cell production in UHV

The organic layers for our solar cells were vapor-deposited in an UHV chamber at ≈10^{-7} mbar vacuum. A schematic drawing of the vacuum chamber is shown on Figure 5.

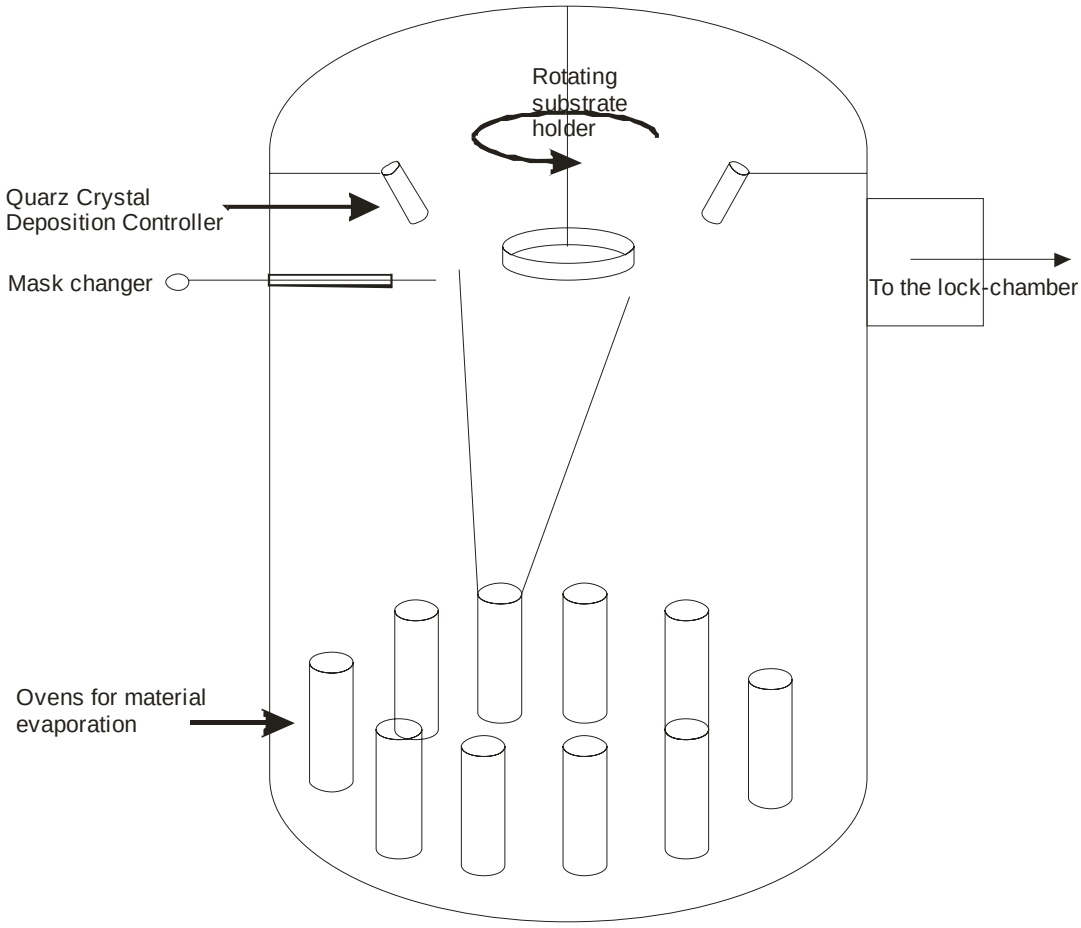

Figure 5. Schematic drawing of the UHV evaporation chamber. Material ovens are situated in the bottom part of the volume, with the opening directed to the sample holder. Rotating substrate holder and deposition controllers are near to each other in the upper part. A mask changer, perpendicular to the sample holder rotation axis, is situated at the level of the mask changing switch on the sample holder

A big cylinder with volume more than 300 liters, the vacuum chamber is kept under UHV through a system of a pre-pump and a turbo pump. The substrate holder enters the UHV chamber through a lock chamber connected to the main one with a vent.

On the side of the lock chamber is shown a manipulator, with which, after evacuation of the lock chamber, the substrate holder is transferred to the main chamber.

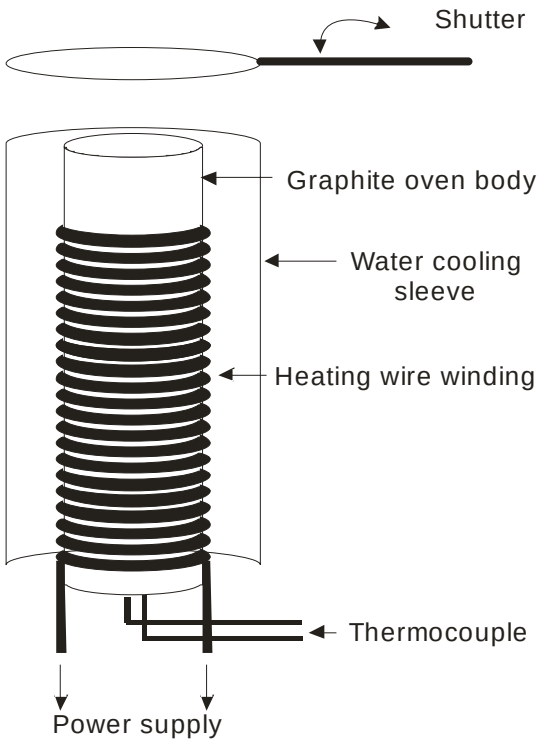

Figure 6. Evaporation oven sketch, illustrating: vertical graphite oven body, heater winding, thermocouple for temperature control and water cooling sleeve

The chemical substances undergoing evaporation are situated in 12 graphite ovens distributed in a circle on the main chamber bottom. Each oven (Figure 6) has a tantalum heater and a water cooling system, connected so, that the heater will only heat the particular oven and nothing else around itself. This way no contamination from walls or bottom can land into the substance vapor flow. The ovens are positioned vertically with the opening on top, facing directly the substrate holder. Evaporation is only possible with an open oven shutter, controlled pneumatically. For the different substances, different evaporation temperatures are used. Temperature is electronically controlled using a metallic thermocouple.

Table 1 shows the approximate evaporation temperature, needed for about 1 Å/s flow, of each substance in the cell.

	ZnPc	C_{60}	BCP	Al electrode
Temperature [°C]	480	550	200	1250

Table 1. Approximate UHV-evaporation temperatures needed for about 1 Å/s flow of the substances, used in organic solar cell production

The ITO substrates are placed in a substrate holder with evaporation mask, having space for 4 samples. The evaporation mask has two positions – for the organics and Al electrodes, between which the switching is done in-situ using a mask changer shaft. The substrate holder is then placed in a rotating head, so that it turns with a defined speed at all times during evaporation. This ensures homogenous growth of the deposited layer. The rotating head is equipped with a heater, so substrates can be heated up to 200 degrees if needed.

Next to the rotating head, quartz crystal deposition controllers (QCDC) are situated. Their function is to monitor the thickness of the layer deposited for each substance and the deposition speed. More on the calibration of QCDC will be said in 3.4.

One evaporation of a complete cell takes approximately one hour, having in mind that the ovens are being kept at parking temperatures. Only for evaporation they are heated to working temperature, which takes time if one does not want to exceed the working temperature by much and partially decompose the substance in the oven. If this happens, then the chemicals are contaminated and have to be renewed, in order to retain reproducibility of the results. For ZnPc and C_{60} the parking temperatures are 200°C, for BCP - 100°C and for Al - 700°C.

After all layer evaporation, the complete cell is transferred through the lock chamber to a glove box. There under nitrogen gas each cell is being securely protected, from atmosphere and humidity, in a specially prepared plexiglas encapsulation. In this form the cells can be taken out of the glove box and their I/V characteristics measured under a sun simulator. In encapsulated state, degradation of the cells takes place in about 5-6 hours.

2.8 Electrical characterization of solar cells

The most widely used method for solar cell characterization is the current-voltage characteristic of the cells, or the so called I/V measurement. It provides very important electrical properties of the cell, from which one can judge how the cell parameters have to be further changed, in order to achieve higher efficiency in sun-light harvesting. The I/V characteristic is influenced by the conductivity of materials and interfaces, exciton or charge carrier diffusion lengths, traps and recombination.

The most important parameter for evaluation of the performance of a solar cell is the efficiency (η). It is defined as the ratio of the maximal electrical power (P_{max}), the cell produces, to the light power received from it (P_{light}):

$$\eta = \frac{P_{max}}{P_{light}}$$

Solar cells are practically diodes, on the contacts of which, under illumination a potential difference could be detected. If the electrical circuit is closed with a resistance, current will flow. The measurement of their I/V characteristics is done the following way: during illumination, a voltage is applied on the electrodes of the cell and the flowing current is measured. The current is divided by the exact cell surface, thus normalized to 1 cm^2, for easier comparison of the results. After normalization the current I (in volts), is referred to, as J (in A/cm^2). A typical I/V curve is shown in Figure 7.

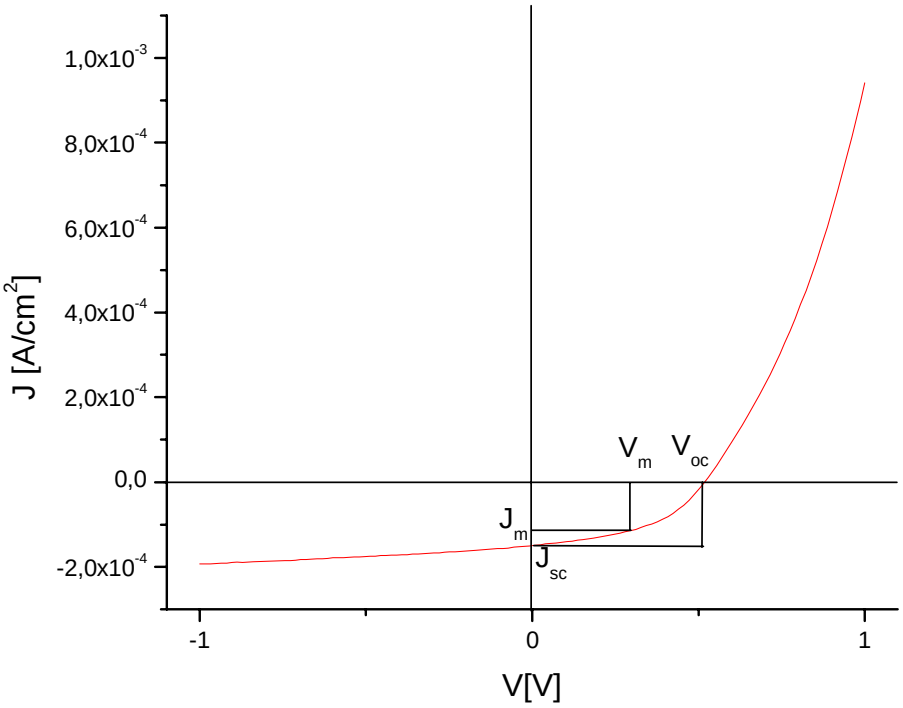

Figure 7. A typical Current/Voltage characteristic for a solar cell.
The clue points are: V_{oc} – open circuit voltage, J_{sc} – short circuit current, V_m – voltage at the point of maximal cell power, J_m – current at the point of maximal cell power

The electrical power of the cell is the product of current and voltage. At one point of the I/V curve the electrical power has a maximum. This is the point with current and voltage marked as J_m and V_m, respectively. Exactly their product gives P_{max} of the cell.

On the I/V curve there are two other important points V_{oc} and J_{sc}. J_{sc} is called short circuit current and is the point where the curve cuts the Y axis. There the applied external voltage turns zero i.e. changes direction. In this point the measured current is entirely the current yielded by the solar cell if its electrodes were short-circuited (from there “sc”).

The second clue point, the open circuit voltage (V_{oc}) is the intersection of the I/V curve with the X axis. There the applied external voltage is exactly equal to the internal voltage of the cell, so no current will flow. These points are the maximal current, respectively voltage that the cell can deliver. In the ideal diode case their product would give the maximal power of the cell, but in reality one more factor is induced: Fill Factor (FF):

$$FF = \frac{I_m.V_m}{I_{sc}.V_{oc}}$$

The fill Factor shows how strong the form of the I/V curve deflects from the curve form of an ideal diode.

The power conversion efficiency of the cell is being calculated using the following equation:

$$\eta[\%] = \frac{FF.I_{sc}V_{oc}}{P_{light}}.100$$

If a solar cell is represented with a replacement circuit (Figure 8) [**30**] then the I/V curve can be fitted with the following formula [**31**,**32**]:

$$I = \frac{I_L - \frac{V}{R_P}}{1+\frac{R_S}{R_P}} - \frac{I_0}{1+\frac{R_S}{R_P}}.(e^{\frac{V - I \cdot R_S}{nkT/q}} - 1)$$

where I is the measured current; I_L – current generated from the cell under illumination; I_0 – reverse current;

This way, two more characteristics could be extracted from the I/V curve. These are the cell's parallel (**R_p**) and serial resistance (**R_s**). The parallel resistance is mainly the slope of the curve in the range around 0V (3rd and 4th quadrant). At lower R_p the open circuit voltage drops, while I_{sc} stays the same.

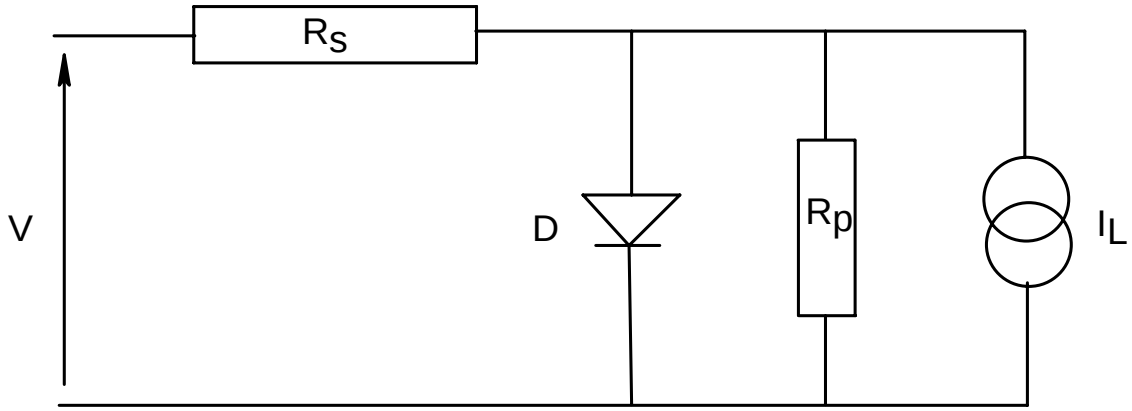

Figure 8. Simplified replacement circuit, a schematic representation of a solar cell.

The serial resistance defines the slope of the I/V curve in 1st quadrant i.e. in the range above the V_{oc} (transmitting direction of diode). Bigger R_s influences the FF and I_{sc} while the V_{oc} stays intact.

So as described the I/V measurement of a cell gives us very useful information about the cell and its internal contact interfaces. That is why every single cell modification described in the present work is accompanied by an I/V curve.

2.9 X-ray reflection [33]

With x-ray reflection, in the present work, layer thickness and structure profile measurements were conducted. A complex method with high requirements, the x-ray reflection provides almost angstrom exact layer thickness measurements. The theory, necessary for understanding the x-ray reflection measurement results in this dissertation, is described here.

In any scattering or reflectivity measurement it is important to distinguish between species of interest and the surrounding medium. This can be represented as a variation in the refractive index **n.** It can be written:

$$n = 1 - \delta + i\beta$$

where δ is the real part of the refractive index and β is the imaginary component which accounts for absorption. For x-rays:

$$\delta = \frac{\lambda^2 \rho_{el} r_0}{2\pi} \text{ and } \beta = \frac{\mu\lambda}{4\pi}$$

where λ is the x-ray wavelength ($\lambda \sim 1{,}5$ Å), ρ_{el} the electron density, r_0 the classical electron radius ($2{,}82.10^{-13}$ cm) and μ the linear absorption coefficient. β depends on the interaction of the incident photons with the electrons in the sample. Experimentally, it is the total absorption cross-section that is of importance. Therefore a strongly scattering sample or a sample with large incoherent scattering cross-section will effectively attenuate the radiation as well. In the calculation of reflectivity this has to be taken into account in β.

For x-rays, contrast or differences in the refractive index, can arise from variations in the mass density. The contrast is provided by the presence of higher atomic number elements, where the number of electrons per unit volume can be large.

In vacuum, the component of the wave vector normal to the surface is given by:

$$Q_{z,0} = \frac{2\pi}{\lambda} \sin\theta$$

where θ is the grazing incidence angle. The subscript *z* denotes the direction normal to the surface of the film and the subscript *0* denotes vacuum. If the reflected x-rays are measured at an angle equal to the incidence angle, the diffraction vector is oriented normal to the surface, i.e. in the *z* direction. In a medium with an x-ray scattering length density $\rho^s=\rho_{el}r_0$, the scattering vector in the medium is modified such that:

$$Q_{z,i} = \sqrt{Q_{z,0} - 4\pi\rho^s} = \sqrt{Q_{z,0}^2 - Q_c^2}$$

where Q_c is the critical scattering vector, which is given by $Q_c = \sqrt{2\delta}$.

It is the change of the scattering vector from one medium to another, that rises reflectivity. This may occur at an interface between two dissimilar materials or from a continuous change in the scattering length density. In either case, a gradient in the scattering length density is required to reflect the radiation. The reflection coefficient at an interface between two media, *i* and *i+1* is given by:

$$r_{i,i+1} = \frac{Q_{z,i} - Q_{z,i+1}}{Q_{z,i} + Q_{z,i+1}}$$

The reflectivity is then given by: $R = r^* r$, where *r** is the complex conjugate for *r*.

In the case of a substrate with a film on it, having a thickness *d* and uniform scattering length density, there are two step changes in the reflection coefficients, at the air/film and film/substrate interfaces, separated by a distance *d*. The reflection coefficient of the sample, in terms of the reflection coefficients at the substrate/sample interface $r_{1,2}$ and at the sample/air interface, $r_{0,1}$ can be written as:

$$r = \frac{r_{0,1} + r_{1,2}\exp(2iQ_{z,1}d)}{1 + r_{0,1}r_{1,2}\exp(2iQ_{z,1}d)}$$

The reflectivity can be shown to be:

$$R(Q_{z,0}) = \frac{r_{0,1}^2 + r_{1,2}^2 + 2r_{0,1}r_{1,2}\cos(2Q_{z,1}d)}{1 + r_{0,1}^2 r_{1,2}^2 + 2r_{0,1}r_{1,2}\cos(2Q_{z,1}d)}$$

From the last equation it is seen, that for a single film, the reflectivity profile as a function of $Q_{z,0}$ will contain oscillations, that are a characteristic of the total film thickness. The "exact" film thickness is given by $\pi/\Delta Q_{z,1}$, where $\Delta Q_{z,1}$ is the distance between two oscillation peak maxima and it can be easily extracted from the R(Q) plot.

2.10 Ellipsometry [34,35,36]

Ellipsometry measures the change in polarization state of light, reflected from the surface of a sample. The measured quantities in ellipsometry are Ψ and Δ, which are related to the ratio of the Fresnel reflection coefficients r_p and r_s for parallel (index *p*) and perpendicular (index *s*) to the plane of incidence polarized light, the following way:

$$\rho = \frac{r_p}{r_s} = \tan\Psi e^{i\Delta}$$

where ρ is the complex reflectance ratio.

There are two independent parameters (Ψ and Δ) for each measurement, which can allow the determination of material properties, with the addition of tighter constraints on the results. Both terms, measured in ellipsometry, relate to a ratio of two values, which make ellipsometry measurements insensitive to fluctuating light intensity, electronic drift, or scattered light loss. In addition, the phase quantity 'Δ' provides excellent sensitivity to the presence of very thin films. For these reasons, ellipsometers can be very accurate and highly reproducible.

Since Ψ and Δ are functions of the complex refractive index: $\tilde{n} = n + ik$ (*n* is the refractive index and *k* the extinction coefficient) they do not directly provide information on the measured film. In order to extract the information contained in the ellipsometric spectra a model describing the structure of the sample and its optical response is usually applied. Only after these fit to a model, the refractive index and film thickness can then be determined.

In a fitting procedure of the experimental spectra, by a variation of the parameters contained in different models, the "Mean Square Error" (MSE) is used, as measure for the deviation between measured values and modeled data.

$$\mathrm{MSE} = \sqrt{\frac{1}{2N-M}\sum_{i=1}^{N}\left[\left(\frac{\Psi_i^{\mathrm{mod}}-\Psi_i^{\mathrm{exp}}}{\sigma_{\Psi,i}^{\mathrm{exp}}}\right)^2+\left(\frac{\Delta_i^{\mathrm{mod}}-\Delta_i^{\mathrm{exp}}}{\sigma_{\Delta,i}^{\mathrm{exp}}}\right)^2\right]}$$

Here N is the number of experimental (Ψ, Δ) pairs, M is the number of variable parameters in the model and σ is the standard deviation on the experimental data points.

Ellipsometry measurements are typically performed at oblique angles near the Brewster condition. This provides the highest sensitivity to material properties, such as refractive index and film thickness. The Brewster condition is different for each sample and also changes over the spectral range. Thus, variable angle of incidence allows the measurement to be optimized for each data point.

Variable angle of incidence also allows measurements at multiple angles. Each new angle will change the path-length of the light traveling through the materials. This can be very beneficial for multi-layers, as different path lengths often lead to new information about the structure. Multiple angles are helpful to improve the confidence in results.

For measurement accuracy an AutoRetarder is used. The AutoRetarder consists of a computer-controlled MgF_2 Berek waveplate, which forms a compensator in the optical path. It is used to improve measurement of the phase quantity ‘Δ’, which can be unambiguously determined over its full range of 360°. The AutoRetarder can also distinguish unpolarized light from circularly polarized light. This is very useful for quantifying the measurement and sample effects. Depolarization of the light beam can be caused from a non-uniform film, backside reflections from a transparent substrate, spatial incoherence of a patterened film, or from the spectral resolution. A spectral measurement of depolarization can help quantify these effects.

2.11 Kelvin Probe Force Microscopy (KPFM) [37,38]

Kelvin probe force microscopy (KPFM) is a powerful technique, used to measure surface topology and contact potential variations, with an atomic force microscope (AFM), on a nanometer scale. Preparation and examination of the surfaces is done in ultrahigh vacuum (UHV). Lateral resolution of the method is ca. 10 nm and vertical resolution is 1 nm. Laser λ is 675 nm.

KPFM is a non-contact AFM operation mode in which the electrostatic interaction is minimized by application of an appropriate bias voltage during topographic imaging. For metals this voltage corresponds to the local work function difference, between sample and tip contact potential difference, whereas for insulators it gives information about the surface charge. The use of KPFM offers the advantage that not only the true topography is recorded, but also a map of the surface potential distribution is acquired.